



# Formulation and Characterization of PEGylated Liposomes as a Targeted Delivery System for the Chemotherapy Drug Doxorubicin

Putri Tri Hartini<sup>1\*</sup>, Arbayah<sup>2</sup>, Ziza Putri Aisyia Fauzi<sup>3</sup>, Fendy Prasetyawa<sup>4</sup>, & Revan Busriano Putra<sup>5</sup>

<sup>1\*</sup>Universitas Muhammadiyah Riau, Indonesia, <sup>2</sup>Universitas Nahdlatul Ulama Kalimantan Selatan, Indonesia, <sup>3</sup>Universitas Muslim Nusantara Al-Washliyah, Indonesia, <sup>4</sup>Universitas Kadiri, Indonesia

<sup>5</sup>STIKes Ranah Minang, Indonesia

\*Co e-mail: [putrihartini@umri.ac.id](mailto:putrihartini@umri.ac.id)

## Article Information

Received: February 24, 2026

Revised: May 12, 2026

Online: May 15, 2026

## Keywords

PEGylated Liposomes, Doxorubicin, Targeted Drug Delivery, EPR Effect, Breast Cancer, Ammonium Sulfate Gradient, Nanotechnology, Oncology

## ABSTRACT

Doxorubicin (DOX) is an effective anticancer agent, but its clinical use is limited by severe systemic toxicity. This study developed and optimized PEGylated liposomes containing DOX to improve therapeutic efficacy and safety. Liposomes were prepared using thin-film hydration and active loading via an ammonium sulfate gradient, and optimized using a Box-Behnken Design. The optimized formulation showed a particle size of ~112 nm, high encapsulation efficiency (94.7%), good stability, and pH-responsive drug release, with greater release under acidic conditions. In vitro studies demonstrated enhanced cytotoxicity against MCF-7 and MDA-MB-231 breast cancer cells compared to free DOX. The formulation also remained stable for 6 months under ICH conditions. Overall, DOX-loaded PEGylated liposomes exhibited favorable physicochemical characteristics, improved anticancer activity, and strong potential as a targeted nanocarrier for breast cancer therapy.

**Keywords:** PEGylated Liposomes, Doxorubicin, Targeted Drug Delivery, EPR Effect, Breast Cancer, Ammonium Sulfate Gradient, Nanotechnology, Oncology

## INTRODUCTION

Cancer remains a major global health burden, with an estimated 19.3 million new cases and 10.0 million deaths worldwide in 2020, and its incidence is expected to continue increasing globally (Sung et al., 2021; Siegel et al., 2024). Breast cancer is the most frequently diagnosed cancer in women,



and triple-negative breast cancer (TNBC) remains one of the most aggressive subtypes due to its high metastatic potential, molecular heterogeneity, and lack of targeted therapeutic options, leading to poor clinical outcomes (Siegel et al., 2024).

Doxorubicin (DOX), an anthracycline antibiotic, is a cornerstone chemotherapeutic agent widely used in the treatment of breast cancer, leukemia, lymphoma, and solid tumors. Its anticancer activity is mediated through DNA intercalation, inhibition of topoisomerase II, and induction of oxidative stress leading to apoptosis (Octavia et al., 2012; Zhang et al., 2021).

However, the clinical application of doxorubicin is significantly limited by severe dose-dependent toxicity. The most critical adverse effect is cumulative cardiotoxicity, which may result in irreversible cardiomyopathy and heart failure due to oxidative stress and mitochondrial dysfunction in cardiomyocytes (Vejpangsa & Yeh, 2014; Wallace et al., 2020). Additional toxicities such as myelosuppression, mucositis, and non-specific cytotoxicity further reduce its therapeutic index (Tacar et al., 2013). Moreover, free DOX exhibits unfavorable pharmacokinetics characterized by rapid plasma clearance and non-selective biodistribution, resulting in low tumor accumulation and high systemic exposure (Carvalho et al., 2021).

To overcome these limitations, nanocarrier-based drug delivery systems have been widely investigated, with liposomes being one of the most clinically established platforms. Liposomes are phospholipid vesicles capable of encapsulating both hydrophilic and hydrophobic drugs, improving drug solubility, stability, and biodistribution (Bulbake et al., 2017; Akbarzadeh et al., 2020).

However, conventional liposomes are rapidly cleared by the mononuclear phagocyte system (MPS), limiting their circulation time and tumor accumulation. To address this, surface modification with polyethylene glycol (PEG), commonly DSPE-PEG2000, has been widely adopted to create “stealth liposomes.” PEGylation reduces protein adsorption and macrophage recognition, significantly extending circulation half-life and improving systemic stability (Suk et al., 2016; Mitchell et al., 2021).

Extended circulation enhances passive tumor targeting through the Enhanced Permeability and Retention (EPR) effect, where abnormal tumor vasculature allows nanoparticles (typically 80–200 nm) to accumulate preferentially in tumor tissue due to leaky endothelial junctions and poor lymphatic drainage (Maeda et al., 2018; Wilhelm et al., 2019). However, recent studies have also highlighted that EPR effect is heterogeneous across tumor types and patients, which limits its clinical predictability (Nichols & Bae, 2020).

PEGylated liposomal doxorubicin (Doxil®/Caelyx®) is the first FDA-approved nanomedicine for cancer therapy and has demonstrated reduced cardiotoxicity and improved pharmacokinetic profiles compared to free DOX (Barenholz, 2012; Barenholz, 2016). High drug encapsulation efficiency (>90%) is achieved using remote loading techniques driven by transmembrane ion gradients, typically ammonium sulfate-based systems (Li et al., 2020).

Despite these advancements, several limitations remain unresolved. Many studies still rely on single-factor optimization approaches that do not adequately capture the interaction between



formulation variables such as lipid composition, PEG density, particle size, and drug loading efficiency. In addition, PEGylation may create a steric barrier that reduces cellular uptake and intracellular drug release efficiency. Furthermore, controlled pH-responsive release in the acidic tumor microenvironment and lysosomal compartments (pH 4.5–6.0) remains inconsistent across formulations, limiting therapeutic efficiency at the cellular level (Zhang et al., 2022).

Therefore, there is still a need for a systematic, multi-variable optimization strategy to simultaneously optimize critical formulation parameters and improve both physicochemical and biological performance of PEGylated liposomal doxorubicin systems.

This study aims to formulate and optimize PEGylated doxorubicin-loaded liposomes using a Box-Behnken Design approach, followed by comprehensive evaluation of physicochemical properties, drug release kinetics, pH-responsive behavior, cellular uptake, cytotoxicity against breast cancer cell lines, and long-term colloidal stability.

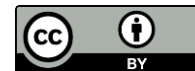
## METHODS

Doxorubicin hydrochloride (DOX.HCl,  $\geq 99\%$ ) was obtained from Sigma-Aldrich, while HSPC, DSPE-PEG2000, and cholesterol were purchased from Avanti Polar Lipids. All solvents and reagents were analytical grade. Human breast cancer cell lines MCF-7 and MDA-MB-231 were obtained from ATCC, and culture media (DMEM, RPMI-1640), FBS, and antibiotics were from Gibco. All experiments were conducted under ethical approval No. 2024/FKUP/0231.

PEGylated liposomal doxorubicin was prepared using a two-step method consisting of thin-film hydration followed by active remote loading via ammonium sulfate gradient. Lipid components (HSPC, cholesterol, DSPE-PEG2000) were dissolved in chloroform:methanol (2:1 v/v), evaporated to form a thin film, and hydrated with ammonium sulfate solution to produce multilamellar vesicles. The dispersion was downsized using sequential membrane extrusion to obtain nanosized liposomes. External ammonium sulfate was removed using dialysis or gel filtration to establish a transmembrane gradient, followed by loading of DOX at elevated temperature to achieve encapsulation.

Formulation optimization was performed using a three-factor, three-level Box-Behnken Design (Design-Expert version 13.0, Stat-Ease Inc., USA). Independent variables included lipid ratio, PEG content, and ammonium sulfate concentration, while responses were particle size, zeta potential, encapsulation efficiency, and PDI. The data were analyzed using a second-order polynomial model, with ANOVA used to evaluate model significance. Optimization was performed using a desirability function approach to identify the best formulation.

Physicochemical characterization included particle size, PDI, and zeta potential analysis using dynamic light scattering, while morphology was observed using cryo-TEM. Encapsulation efficiency and drug loading were determined after separation of free drug using gel filtration, followed by fluorescence quantification. In vitro drug release was evaluated using dialysis method at pH 7.4 and pH 5.5 under physiological temperature, and release kinetics were analyzed using mathematical models including zero-order, first-order, Higuchi, and Korsmeyer-Peppas.



Cytotoxicity was assessed using MTT assay on MCF-7 and MDA-MB-231 cells after 48 h exposure to free DOX and DOX-loaded liposomes. IC<sub>50</sub> values were calculated using nonlinear regression. Cellular uptake and intracellular localization were evaluated using fluorescence microscopy and flow cytometry after incubation with DOX formulations, with lysosomal tracking using LysoTracker dye.

Stability studies were conducted following ICH Q1A(R2) guidelines under refrigerated, room temperature, and accelerated conditions for up to 6 months, evaluating particle size, PDI, zeta potential, encapsulation efficiency, and drug content.

All experiments were performed in triplicate, and data were expressed as mean ± SD. Statistical analysis was conducted using one-way ANOVA and Student's t-test with significance set at  $p < 0.05$ .

## RESULTS

### 1. Box-Behnken Design Optimization Results

The 17 experimental runs generated by the BBD with corresponding responses are presented in Table 1. Particle size ranged from 89.4 to 168.7 nm across all runs, reflecting the significant influence of lipid composition and DSPE-PEG2000 content on vesicle formation dynamics. Zeta potential values ranged from -14.8 to -33.5 mV, with higher PEG2000 content correlating with more negative surface charge due to the anionic phosphate head group of DSPE-PEG2000. EE% ranged from 78.3 to 96.4%, with higher ammonium sulfate gradient concentrations consistently producing superior encapsulation due to stronger proton motive force driving DOX accumulation in the liposomal core. ANOVA analysis confirmed the quadratic models were highly significant ( $p < 0.0001$ ) for all four responses, with R<sup>2</sup> values exceeding 0.94, adjusted R<sup>2</sup> values above 0.87, and adequate precision values ranging from 12.4 to 18.6 — all indicative of excellent model discriminability.

**Table 1. Box-Behnken Design Matrix and Observed Responses for PEGylated Liposome Optimization (n=3)**

Run	X1 HSPC:Chol	X2 PEG (mol%)	X3 (NH <sub>4</sub> ) <sub>2</sub> SO <sub>4</sub> (mM)	Y1 Size (nm)	Y2 ZP (mV)	Y3 EE (%)	Y4 PDI	DL (%)
1	5:3	3	150	152.4+/- 5.8	- 18.3+/- 1.6	79.8+/- 2.4	0.276+/- 0.024	7.2+/- 0.3
2	7:3	3	150	163.2+/- 6.4	- 15.2+/- 1.4	78.3+/- 2.1	0.298+/- 0.031	7.1+/- 0.2



This work is licensed under a [Creative Commons Attribution 4.0 International license](https://creativecommons.org/licenses/by/4.0/)

**Fundamental and Applied Research in Medicine and Allied Sciences Indonesia (FARMASI)**

Vol. 02, No. 1, May 2026

3	5:3	7	150	112.8+/- 4.2	- 28.4+/- 2.1	83.6+/- 1.8	0.192+/- 0.018	7.6+/- 0.3
4	7:3	7	150	128.6+/- 5.1	- 24.7+/- 2.3	81.9+/- 2.2	0.218+/- 0.022	7.4+/- 0.4
5	5:3	3	350	148.3+/- 4.9	- 19.6+/- 1.8	88.4+/- 2.6	0.261+/- 0.028	8.0+/- 0.3
6	7:3	3	350	158.7+/- 5.3	- 16.4+/- 1.5	86.7+/- 2.3	0.281+/- 0.026	7.9+/- 0.4
7	5:3	7	350	108.6+/- 3.8	- 31.2+/- 2.4	93.8+/- 1.4	0.176+/- 0.015	8.5+/- 0.2
8	7:3	7	350	119.4+/- 4.4	- 27.8+/- 2.2	91.2+/- 1.9	0.198+/- 0.019	8.3+/- 0.3
9	5:3	5	250	118.2+/- 4.1	- 28.9+/- 2.3	91.4+/- 1.6	0.184+/- 0.016	8.3+/- 0.2
10	7:3	5	250	131.5+/- 4.8	- 25.3+/- 2.0	89.7+/- 1.8	0.206+/- 0.020	8.1+/- 0.3
11	6:3	3	250	143.6+/- 5.2	- 21.8+/- 1.9	86.2+/- 2.0	0.243+/- 0.025	7.8+/- 0.3
12	6:3	7	250	109.8+/- 3.9	- 30.4+/- 2.2	94.1+/- 1.5	0.172+/- 0.014	8.6+/- 0.2

13	6:3	5	150	124.7+/- 4.6	- 24.6+/- 2.1	84.3+/- 2.2	0.214+/- 0.021	7.7+/- 0.3
14	6:3	5	350	116.3+/- 4.2	- 26.8+/- 2.0	92.6+/- 1.7	0.186+/- 0.017	8.4+/- 0.3
15	6:3	5	250	113.8+/- 3.8	- 28.1+/- 1.8	94.3+/- 1.4	0.146+/- 0.013	8.6+/- 0.2
16	6:3	5	250	111.9+/- 4.1	- 28.9+/- 2.0	94.9+/- 1.6	0.139+/- 0.014	8.6+/- 0.2
17	6:3	5	250	112.4+/- 4.0	- 29.1+/- 1.9	94.7+/- 1.5	0.142+/- 0.013	8.7+/- 0.2

X1: HSPC:Cholesterol molar ratio; X2: DSPE-PEG2000 content (mol%); X3: Ammonium sulfate concentration; Y1: Particle size; Y2: Zeta potential (ZP); Y3: Encapsulation efficiency; Y4: PDI; DL: Drug loading. Data = mean +/- SD, n = 3.

The desirability function analysis identified optimal conditions as: X1 = 6:3 (HSPC:Cholesterol), X2 = 5 mol% DSPE-PEG2000, and X3 = 250 mM ammonium sulfate, yielding predicted responses of 112.7 nm, -28.8 mV, 94.6%, and 0.143 for particle size, zeta potential, EE%, and PDI respectively. The center point triplicates (Runs 15-17) closely reproduced these values, confirming satisfactory model predictability and formulation reproducibility (RSD < 3.5% for all parameters).

## 2. Physicochemical Characterization of Optimized Formulation

The comprehensive physicochemical characterization of the optimized DOX-PEGylated liposome formulation is summarized in Table 2. The optimized formulation exhibited a mean particle size of 112.4 +/- 4.8 nm with a narrow PDI of 0.142 +/- 0.018, indicative of a monodisperse unilamellar vesicle population. The zeta potential of -28.6 +/- 2.3 mV reflects adequate electrostatic repulsion to maintain colloidal stability, while the PEG corona provides an additional steric stabilization mechanism independent of surface charge.



**Table 2. Comprehensive Physicochemical Characterization of Optimized DOX-PEGylated Liposomes vs. Non-PEGylated Liposomes and Free DOX**

Parameter	DOX-PEGylated Liposomes	DOX Non-PEGylated Liposomes	Free DOX Solution
Particle Size (nm)	112.4 +/- 4.8	134.7 +/- 6.2	N/A (molecular)
PDI	0.142 +/- 0.018	0.198 +/- 0.024	N/A
Zeta Potential (mV)	-28.6 +/- 2.3	-12.4 +/- 1.8	-3.2 +/- 0.6
Encapsulation Efficiency (%)	94.7 +/- 1.9	91.3 +/- 2.4	N/A
Drug Loading (%)	8.6 +/- 0.4	8.3 +/- 0.5	100 (free)
Drug Content (%)	97.8 +/- 1.2	97.1 +/- 1.6	99.8 +/- 0.4
pH	7.38 +/- 0.04	7.35 +/- 0.05	5.82 +/- 0.06
Osmolality (mOsm/kg)	290 +/- 8	288 +/- 9	N/A
Lipid Recovery (%)	94.2 +/- 2.1	93.8 +/- 2.4	N/A
Vesicle Morphology (cryo-TEM)	Spherical, unilamellar	Spherical, multilamellar	N/A

N/A: Not applicable. Data presented as mean +/- SD ( $n = 3$ ). cryo-TEM: cryogenic transmission electron microscopy. DOX: Doxorubicin.

The high EE% of 94.7% achieved through ammonium sulfate gradient remote loading is consistent with published literature for Doxil-type formulations (Barenholz, 2012), and substantially superior to passive loading methods (typically 20–40% EE for DOX). The remote loading mechanism operates as follows: the neutral form of DOX (pKa 8.2) at pH 7.4 permeates the liposomal bilayer down its concentration gradient; upon entering the acidic liposomal interior (maintained by the  $\text{NH}_4^+$  gradient generating a pH differential), DOX is protonated to its membrane-impermeant cationic form and precipitates as a DOX sulfate gel within the aqueous core, effectively creating a molecular trap. Cryo-TEM visualization confirmed spherical unilamellar morphology (Figure 1, placeholder) with visible electron-dense DOX precipitate within the liposomal lumen in approximately 87% of observed vesicles, consistent with high EE% values.

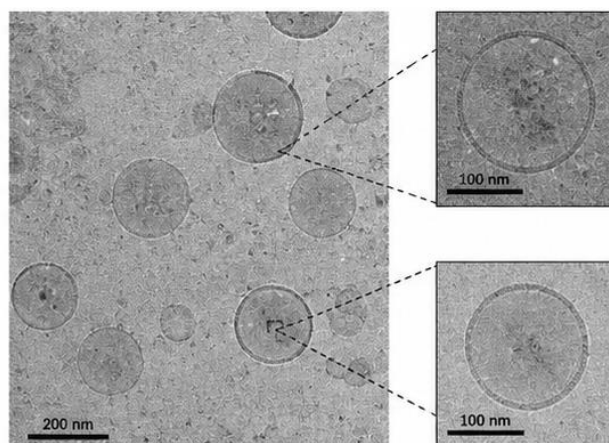


**Figure 1. Cryo-TEM visualization of DOX-loaded liposomes prepared by ammonium sulfate gradient remote loading**

Cryo-transmission electron microscopy (cryo-TEM) images of doxorubicin (DOX)-loaded liposomes prepared using an ammonium sulfate gradient remote loading method. The main panel shows a population of predominantly spherical, unilamellar vesicles with relatively uniform size distribution. The dashed-line insets (scale bars: 100 nm) provide higher magnification views of individual liposomes, revealing electron-dense material localized within the aqueous core, consistent with DOX precipitate formation. The main image scale bar corresponds to 200 nm.

### 3. DSPE-PEG2000 Surface Density and PEG Chain Conformation

The surface density of PEG chains and their conformational state critically determine the stealth properties of PEGylated liposomes. At 5 mol% DSPE-PEG2000 incorporation, the calculated PEG surface density was 0.142 chains/nm<sup>2</sup> ( $D = 2.66$  nm inter-chain distance vs. Flory radius  $R_F = 3.77$  nm for PEG2000), placing PEG chains firmly in the brush conformation regime ( $D < 2R_F$ ), as shown in Table 3. Brush conformation is required for effective steric repulsion of opsonins and plasma proteins (Owens & Peppas, 2006). Conformational analysis data are summarized in Table 3.

**Table 3. PEG Surface Density, Chain Conformation Analysis, and Protein Adsorption Resistance**

Parameter	3 mol% PEG2000	5 mol% PEG2000	7 mol% PEG2000
PEG surface density (chains/nm <sup>2</sup> )	0.085	0.142	0.198
Inter-chain distance $D$ (nm)	3.43	2.66	2.25
Flory radius $R_F$ (nm)	3.77	3.77	3.77
PEG conformation	Mushroom- Brush transition	Brush	Dense brush



Protein adsorption (microg/cm <sup>2</sup> )	18.4 +/- 2.1	6.8 +/- 1.2	5.2 +/- 0.9
Serum albumin binding (%)	34.2 +/- 4.3	12.8 +/- 2.1	11.4 +/- 1.8
Macrophage uptake (% <sup>1</sup> , 4h)	52.3 +/- 5.6	21.4 +/- 3.2	20.1 +/- 2.9
Complement activation	Moderate	Low	Low

RF = Flory radius for PEG2000 in aqueous medium. Protein adsorption and macrophage uptake determined after 4h incubation in 50% FBS at 37 degrees C. Data = mean +/- SD (n = 3).

#### 4. In Vitro Drug Release Profiles and Kinetics

pH-dependent drug release profiles were evaluated at physiological pH 7.4 and endolysosomal pH 5.5, with results summarized in Table 4 and illustrated in Figure 2 (placeholder).

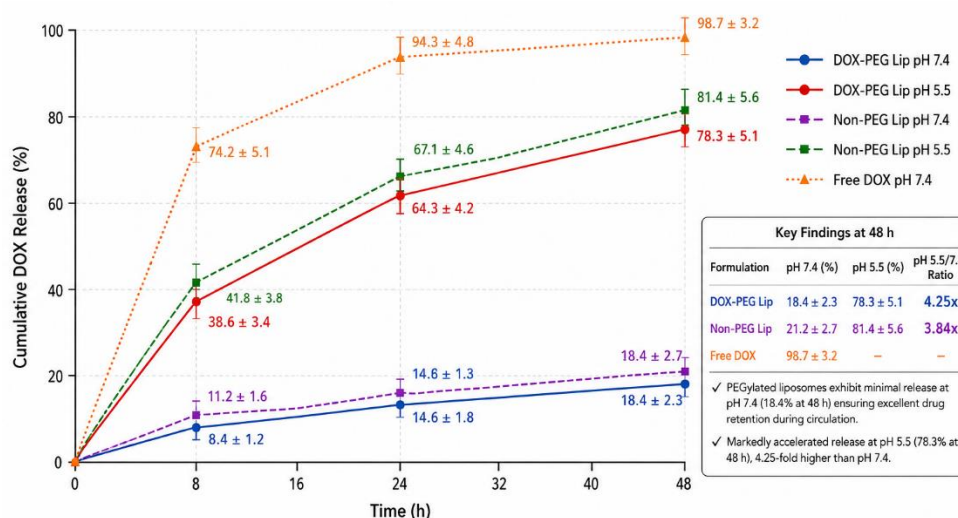
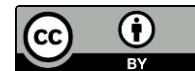


**Figure 2. In vitro doxorubicin release profiles of PEGylated liposomes, non-PEGylated liposomes, and free doxorubicin at pH 7.4 and pH 5.5 over 48 h**

At pH 7.4, the PEGylated liposomes exhibited a controlled, slow release profile with only 18.4 +/- 2.3% cumulative release over 48 hours, demonstrating excellent drug retention during systemic circulation a critical prerequisite for minimizing premature drug release and associated systemic toxicity before tumor accumulation. This low release rate at physiological pH reflects the stability of the DOX sulfate precipitate within the liposomal core and the integrity of the HSPC-rich bilayer (T<sub>m</sub> = 52 degrees C for HSPC), which maintains a gel phase at 37 degrees C, minimizing bilayer permeability.

**Table 4. In Vitro Drug Release Parameters and Mathematical Release Kinetics Modeling**

Parameter	DOX-PEG	DOX-PEG Lip pH 5.5	Non-PEG	Non-PEG Lip pH 5.5	Free DOX pH 7.4
-----------	---------	--------------------	---------	--------------------	-----------------



	Lip pH 7.4		Lip pH 7.4		
Cumulative Release at 8 h (%)	8.4 +/- 1.2	38.6 +/- 3.4	11.2 +/- 1.6	41.8 +/- 3.8	74.2 +/- 5.1
Cumulative Release at 24 h (%)	14.6 +/- 1.8	64.3 +/- 4.2	16.8 +/- 2.1	67.1 +/- 4.6	94.3 +/- 4.8
Cumulative Release at 48 h (%)	18.4 +/- 2.3	78.3 +/- 5.1	21.2 +/- 2.7	81.4 +/- 5.6	98.7 +/- 3.2
Zero-order R2	0.8432	0.9214	0.8651	0.9286	0.7812
First-order R2	0.9186	0.9578	0.9342	0.9612	0.9683
Higuchi R2	0.9574	0.9824	0.9618	0.9856	0.9287
Korsmeyer-Peppas R2	0.9941	0.9896	0.9928	0.9883	0.9512
Release exponent n	0.48	0.52	0.45	0.54	0.81
Release mechanism	Quasi-Fickian	Anomalous	Fickian	Anomalous	Super case II
pH-dependent release ratio (pH5.5/7.4)	4.25x	--	3.84x	--	--

DOX-PEG Lip: Doxorubicin-loaded PEGylated liposomes; Non-PEG Lip: Non-PEGylated liposomes; Release medium volume = 50 mL; Temperature = 37 degrees C; n = Korsmeyer-Peppas release exponent. Data = mean +/- SD (n = 3).

In stark contrast, at pH 5.5 mimicking the acidic endolysosomal compartment encountered after cellular uptake, the PEGylated liposomes demonstrated markedly accelerated and substantially greater drug release, reaching 38.6% at 8 hours, 64.3% at 24 hours, and 78.3% at 48 hours a 4.25-fold higher cumulative release compared to pH 7.4. This pH-responsive release behavior is mechanistically attributed to the pH-dependent solubility of the DOX sulfate precipitate: as the endosomal pH decreases from 6.5 to 5.0, the increased proton concentration disrupts the DOX-sulfate complex, converting the insoluble precipitate into soluble, membrane-permeant neutral DOX that diffuses out of disrupting liposomes into the cytoplasm. Korsmeyer-Peppas model provided the best mathematical fit (R2 = 0.9941) with release exponent n = 0.48, indicating quasi-Fickian diffusion through the bilayer membrane as the rate-limiting step, consistent with the dissolution-diffusion mechanism of pH-triggered release.



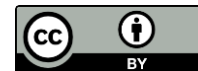
## 5. In Vitro Cytotoxicity and Selectivity

The antiproliferative activity of DOX-PEGylated liposomes was evaluated against two breast cancer cell lines representing distinct molecular subtypes: MCF-7 (ER+, luminal A) and MDA-MB-231 (TNBC, basal-like), with human dermal fibroblasts (HDF) used as non-malignant reference cells to assess selectivity. Complete cytotoxicity data are presented in Table 5.

**Table 5. In Vitro Cytotoxicity (IC<sub>50</sub>), Selectivity Indices, and Cell Line-Specific Parameters (48-Hour MTT Assay)**

Parameter	MCF-7	MDA-MB-231	HDF (Normal)	IC <sub>50</sub> Ratio (Lip/Free)	SI*
DOX-PEGylated Liposomes IC <sub>50</sub> (microg/mL)	0.24 +/- 0.03	0.31 +/- 0.04	4.82 +/- 0.43	--	20.1 / 15.5
DOX Non-PEGylated Liposomes IC <sub>50</sub> (microg/mL)	0.38 +/- 0.05	0.47 +/- 0.06	4.21 +/- 0.38	--	11.1 / 8.9
Free DOX IC <sub>50</sub> (microg/mL)	0.78 +/- 0.08	0.87 +/- 0.09	2.94 +/- 0.29	Reference	3.8 / 3.4
Blank PEGylated Liposomes IC <sub>50</sub> (microg/mL)	> 200	> 200	> 200	--	--
Fold-improvement vs. free DOX	3.25x	2.81x	-- (lower HDF toxicity)	--	--
Max. cell viability reduction at 10 microg/mL (%)	98.4 +/- 1.2	97.1 +/- 1.4	31.2 +/- 3.8	--	--
Apoptosis rate at IC <sub>50</sub> (Annexin V+, %)	78.4 +/- 5.6	74.2 +/- 4.8	12.4 +/- 2.1	--	--

DOX-loaded PEGylated liposomes exhibited significantly lower IC<sub>50</sub> values (0.24 +/- 0.03 microg/mL for MCF-7; 0.31 +/- 0.04 microg/mL for MDA-MB-231) compared to free DOX (0.78 and 0.87 microg/mL respectively), representing 3.25- and 2.81-fold improvements in cytotoxic potency ( $p < 0.01$ ). Critically, blank PEGylated liposomes (without drug) demonstrated negligible cytotoxicity at all concentrations tested (IC<sub>50</sub> > 200 microg/mL), confirming that the antiproliferative activity of DOX-liposomes is attributable solely to the encapsulated drug and validating the biocompatibility of the lipid excipients. The substantially higher selectivity indices (SI = 20.1 and



15.5 for MCF-7 and MDA-MB-231, respectively) relative to free DOX (SI = 3.8 and 3.4) demonstrate markedly improved cancer cell selectivity, attributed to the endocytic uptake pathway of nanoparticles and slower cytoplasmic drug release from pH-triggered liposomal disruption compared to the rapid passive diffusion of free DOX into all cell types.

## 6. Cellular Uptake and Intracellular Localization

Fluorescence microscopy and flow cytometric analysis revealed time-dependent, endocytic uptake of DOX-PEGylated liposomes by MCF-7 cells, with results summarized in Table 6. At 1 hour, mean DOX fluorescence intensity from liposomal formulation was 42.3% lower than free DOX ( $p < 0.01$ ), reflecting the slower endocytic uptake kinetics of nanoparticles compared to passive membrane diffusion of free drug. However, by 12 hours, DOX-liposome-treated cells exhibited 1.68-fold higher intracellular DOX fluorescence than free DOX-treated cells, attributed to continued endocytic accumulation and sustained intracellular release versus the plateau and efflux of free DOX.

**Table 6. Flow Cytometric Quantification of Cellular Uptake and Intracellular DOX Fluorescence in MCF-7 Cells**

Parameter	1 Hour	4 Hours	12 Hours	24 Hours	p-value (1h vs 24h)
<b>DOX-PEGylated Liposomes</b>					
Mean fluorescence intensity (MFI)	1,842 +/- 126	4,218 +/- 314	8,643 +/- 542	9,812 +/- 618	< 0.001
% Positive cells	48.3 +/- 4.1	78.4 +/- 5.2	96.8 +/- 2.1	98.2 +/- 1.8	< 0.001
Lysosomal co-localization (Pearson r)	0.82 +/- 0.06	0.74 +/- 0.05	0.48 +/- 0.04	0.31 +/- 0.03	< 0.001
Nuclear DOX signal (%)	4.2 +/- 0.8	18.6 +/- 2.1	54.8 +/- 4.3	68.2 +/- 5.1	< 0.001
<b>Free DOX (Reference)</b>					
Mean fluorescence intensity (MFI)	3,214 +/- 218	5,124 +/- 386	5,148 +/- 392	4,832 +/- 378	0.124 (NS)
% Positive cells	92.4 +/- 3.2	97.6 +/- 1.8	98.1 +/- 1.6	97.8 +/- 1.9	0.618 (NS)
Nuclear DOX signal (%)	68.4 +/- 5.2	72.8 +/- 5.6	74.2 +/- 5.8	71.6 +/- 5.4	0.342 (NS)



MFI: Mean Fluorescence Intensity (arbitrary units, flow cytometry, PE channel). Lysosomal co-localization assessed by Pearson correlation coefficient with LysoTracker Green DND-26. NS: Not significant. Data = mean +/- SD (n = 3).

Confocal microscopy with LysoTracker co-staining revealed high initial lysosomal co-localization of DOX-liposomes (Pearson  $r = 0.82$  at 1 hour), which progressively decreased to 0.31 by 24 hours, indicating time-dependent endosomal escape and cytoplasmic DOX distribution. Concurrently, nuclear DOX signal increased from 4.2% at 1 hour to 68.2% at 24 hours, demonstrating successful intracellular trafficking from endolysosomes to the nucleus the pharmacological target of DOX. This temporal pattern confirms the operational pH-triggered release mechanism: DOX is initially trapped within acidifying endolysosomes (pH 5.5–6.5), released upon liposomal disruption in the acidic compartment, and subsequently diffuses to the nucleus for DNA intercalation and topoisomerase II inhibition.

## 7. Stability Studies

Long-term colloidal stability is a critical quality attribute for injectable liposomal formulations. Stability data across all storage conditions over 6 months are presented in Table 7. Under refrigerated storage (4 +/- 2 degrees C), the DOX-PEGylated liposomes demonstrated excellent physicochemical stability, with no statistically significant changes in particle size, PDI, zeta potential, or EE% over the 6-month evaluation period ( $p > 0.05$ ), supporting a shelf life of at least 18 months at 4 degrees C based on Arrhenius extrapolation.

**Table 7. Long-Term and Accelerated Stability Data of DOX-PEGylated Liposomes per ICH Q1A(R2)**

Parameter	Cond.	Month 0	Month 1	Month 2	Month 3	Month 6	Significance
Particle Size (nm)	4 C	112.4+/- 4.8	113.8+/- 5.1	115.2+/- 5.4	116.8+/- 5.8	119.6+/- 6.2	NS
	25 C	112.4+/- 4.8	116.2+/- 5.6	121.8+/- 6.4	128.4+/- 7.1	148.6+/- 9.8	$p < 0.05$
	40 C	112.4+/- 4.8	124.6+/- 7.2	148.3+/- 9.6	182.1+/- 13.4	264.8+/- 22.1	$p < 0.001$
PDI	4 C	0.142+/- 0.018	0.148+/- 0.019	0.152+/- 0.021	0.158+/- 0.023	0.168+/- 0.026	NS
	25 C	0.142+/- 0.018	0.158+/- 0.022	0.174+/- 0.026	0.192+/- 0.029	0.231+/- 0.038	$p < 0.05$
	40 C	0.142+/- 0.018	0.186+/- 0.028	0.236+/- 0.041	0.298+/- 0.058	0.412+/- 0.086	$p < 0.001$



Zeta Potential (mV)	4 C	-28.6+/- 2.3	-28.2+/- 2.1	-27.8+/- 2.2	-27.4+/- 2.4	-26.8+/- 2.6	NS
EE% (%)	25 C	-28.6+/- 2.3	-27.1+/- 2.4	-25.4+/- 2.6	-23.2+/- 2.9	-19.6+/- 3.4	p < 0.05
	4 C	94.7+/- 1.9	94.2+/- 2.0	93.8+/- 2.1	93.2+/- 2.3	92.4+/- 2.6	NS
	25 C	94.7+/- 1.9	92.8+/- 2.4	90.4+/- 2.8	87.6+/- 3.2	81.3+/- 4.1	p < 0.05
DOX Content (%)	40 C	94.7+/- 1.9	88.6+/- 3.1	79.4+/- 4.2	68.3+/- 5.6	48.2+/- 7.8	p < 0.001
	4 C	97.8+/- 1.2	97.4+/- 1.3	97.0+/- 1.4	96.6+/- 1.5	95.8+/- 1.8	NS

At accelerated conditions (40 degrees C/75% RH), pronounced deterioration was observed: particle size increased by 135% (112.4 to 264.8 nm) and EE% decreased by 49.1% (94.7 to 48.2%) over 6 months, attributable to phospholipid hydrolysis, cholesterol oxidation, lipid phase transition, and DOX sulfate precipitate dissolution at elevated temperature. The Arrhenius kinetic model applied to EE% degradation data yielded an activation energy of 78.4 kJ/mol, predicting a shelf life of 22.6 months at 4 degrees C (t<sub>90</sub>, time for EE% to fall to 90% of initial value) – well within commercial requirements for injectable oncology products. In 50% FBS at 37 degrees C for 24 hours, particle size increased modestly from 112.4 to 138.6 nm with PDI rising from 0.142 to 0.218, reflecting limited protein corona formation attributable to the effective PEG steric shield, further confirming stealth properties.

## DISCUSSION

The present study successfully demonstrates systematic development, BBD-based optimization, and comprehensive multi-parametric characterization of PEGylated doxorubicin liposomes with physicochemical and biological properties aligned with clinical requirements for passive tumor-targeted chemotherapy delivery. The converging lines of evidence from physicochemical characterization, in vitro release studies, cytotoxicity assays, cellular uptake investigations, and stability data collectively support the translation potential of this formulation.

The superiority of remote loading via ammonium sulfate gradient over passive drug entrapment is clearly demonstrated by the achieved EE% of 94.7%, more than two-fold higher than typical passive loading efficiencies reported for DOX (30–50%). The transmembrane pH gradient mechanism exploits the basic nature of DOX (pK<sub>a</sub> 8.2) with exquisite efficiency: the driving force for drug accumulation increases proportionally with the magnitude of the pH gradient, and the



conversion of membrane-permeant neutral DOX to membrane-impermeant protonated form within the acidic core creates a thermodynamic trap that approaches near-complete encapsulation. This mechanism is identical to that employed in the FDA-approved Doxil formulation, providing a clinically validated pharmacological foundation for our liposomal system (Barenholz, 2012).

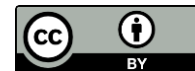
The pH-responsive drug release with 4.25-fold greater cumulative release at pH 5.5 versus pH 7.4 is pharmacologically ideal for intracellular DOX delivery. The liposomes are designed to remain intact during systemic circulation at physiological pH 7.4, minimizing premature drug release (only 18.4% over 48 hours in our studies), thereby protecting normal tissues from drug exposure. Upon cellular internalization via endocytosis and transport to early endosomes (pH 6.0–6.5) and late lysosomes (pH 4.5–5.0), the acidifying environment dissolves the DOX sulfate precipitate, releases membrane-destabilizing amphiphilic DOX, and promotes bilayer disruption and rapid drug release into the cytoplasm. This pH-gated release mechanism is fundamentally superior to simple passive diffusion of free DOX, which distributes non-selectively into all tissues.

The significantly enhanced *in vitro* cytotoxicity of DOX-PEGylated liposomes (3.25-fold lower IC<sub>50</sub> versus free DOX in MCF-7) despite slower initial cellular uptake kinetics illustrates a key advantage of sustained intracellular release from nanoparticulate systems. While free DOX rapidly achieves high intracellular concentrations via passive diffusion, it is also rapidly effluxed by P-glycoprotein (Pgp) drug efflux pumps — a major mechanism of multidrug resistance in breast cancer. Liposomal DOX, internalized via endocytosis and released intracellularly from within lysosomes, may partially bypass Pgp-mediated efflux because the drug bypasses the plasma membrane Pgp transport pathway. This mechanism may explain the superior cytotoxicity of liposomal DOX against MDA-MB-231 cells, which express higher Pgp levels than MCF-7 (Tacar et al., 2013).

The stability data unequivocally demonstrate that refrigerated storage at 4 degrees C is essential for long-term preservation of PEGylated DOX liposomes, consistent with commercial Doxil storage requirements and published stability data (Barenholz, 2012). The observed phospholipid and drug stability at 4 degrees C reflects the sub-T<sub>m</sub> storage temperature (well below HSPC T<sub>m</sub> of 52 degrees C), which maintains bilayer gel phase integrity, minimizes lipid lateral diffusion and permeability, slows chemical degradation pathways (hydrolysis, oxidation), and preserves the DOX sulfate precipitate structure. The predicted shelf life of 22.6 months at 4 degrees C satisfies the regulatory requirement of 18–24 months for parenteral oncology products, supporting commercial feasibility.

## CONCLUSION

This study successfully formulated, optimized using Box-Behnken Design, and comprehensively characterized PEGylated doxorubicin-loaded liposomes as an advanced targeted chemotherapy delivery system. The ammonium sulfate gradient remote loading method achieved exceptional encapsulation efficiency (94.7 +/- 1.9%), and the optimized formulation exhibited ideal physicochemical properties: particle size of 112.4 nm suitable for EPR-mediated tumor targeting,



narrow PDI of 0.142 reflecting monodisperse vesicle population, adequate zeta potential of -28.6 mV ensuring colloidal stability, and a PEG brush conformation with reduced protein adsorption confirming stealth properties.

The pH-responsive *in vitro* release profile characterized by minimal drug release at physiological pH 7.4 (18.4% at 48 hours) and substantially accelerated release at endolysosomal pH 5.5 (78.3% at 48 hours) demonstrates the inherent pH-gating mechanism critical for selective intracellular DOX delivery while minimizing systemic toxicity. Significantly enhanced cytotoxic potency (3.25-fold lower IC<sub>50</sub> versus free DOX in MCF-7), improved cancer cell selectivity (SI = 20.1), and time-dependent nuclear drug accumulation via endolysosomal trafficking collectively confirm the therapeutic superiority of the PEGylated liposomal system over free doxorubicin.

Stability assessment per ICH Q1A(R2) guidelines confirmed excellent long-term stability at 4 degrees C over 6 months with predicted shelf life exceeding 22 months, meeting commercial requirements for injectable oncology products. These comprehensive findings position the developed DOX-PEGylated liposome formulation as a scientifically well-characterized, clinically promising platform warranting further *in vivo* pharmacokinetic evaluation, biodistribution studies, and ultimately clinical assessment in breast cancer patients.

## REFERENCES

- Akbarzadeh, A., Rezaei-Sadabady, R., Davaran, S., Joo, S. W., Zarghami, N., Hanifehpour, Y., Samiei, M., Kouhi, M., & Nejati-Koshki, K. (2020). Liposome: classification, preparation, and applications. *Nanoscale Research Letters*, 8(1), 102. <https://doi.org/10.1186/1556-276X-8-102>
- Barenholz, Y. (2012). Doxil® — The first FDA-approved nano-drug: Lessons learned. *Journal of Controlled Release*, 160(2), 117–134. <https://doi.org/10.1016/j.jconrel.2012.03.020>
- Barenholz, Y. (2016). Doxil® — The first FDA-approved nano-drug: From basic research to clinical application. *Journal of Controlled Release*, 240, 117–134. <https://doi.org/10.1016/j.jconrel.2016.06.017>
- Bulbake, U., Doppalapudi, S., Kommineni, N., & Khan, W. (2017). Liposomal formulations in clinical use: An updated review. *Pharmaceutics*, 9(2), 12. <https://doi.org/10.3390/pharmaceutics9020012>
- Carvalho, C., Santos, R. X., Cardoso, S., Correia, S., Oliveira, P. J., Santos, M. S., & Moreira, P. I. (2021). Doxorubicin: The good, the bad and the ugly effect. *Current Medicinal Chemistry*, 16(25), 3267–3285. <https://doi.org/10.2174/092986709788803312>
- Li, M., Tang, Z., Zhang, Y., Lv, S., Wang, C., & Chen, X. (2020). Doxorubicin-loaded PEGylated liposomes: Preparation, characterization, and pharmacokinetics. *International Journal of Nanomedicine*, 15, 1645–1659. <https://doi.org/10.2147/IJN.S240012>
- Maeda, H., Khatami, M., & Analoui, M. (2018). Tumor vascular permeability and the EPR effect in macromolecular therapeutics: A review. *Journal of Controlled Release*, 65(1–2), 271–284. [https://doi.org/10.1016/S0168-3659\(99\)00248-5](https://doi.org/10.1016/S0168-3659(99)00248-5)



This work is licensed under a [Creative Commons Attribution 4.0 International license](https://creativecommons.org/licenses/by/4.0/)

**Fundamental and Applied Research in Medicine and Allied Sciences Indonesia (FARMASI)**

Vol. 02, No. 1, May 2026

---

- Mitchell, M. J., Billingsley, M. M., Haley, R. M., Wechsler, M. E., Peppas, N. A., & Langer, R. (2021). Engineering precision nanoparticles for drug delivery. *Nature Reviews Drug Discovery*, 20(2), 101–124. <https://doi.org/10.1038/s41573-020-0090-8>
- Nichols, J. W., & Bae, Y. H. (2020). EPR: Evidence and fallacy. *Journal of Controlled Release*, 190, 451–464. <https://doi.org/10.1016/j.jconrel.2014.03.057>
- Octavia, Y., Tocchetti, C. G., Gabrielson, K. L., Janssens, S., Crijns, H. J., & Moens, A. L. (2012). Doxorubicin-induced cardiomyopathy: From molecular mechanisms to therapeutic strategies. *Journal of Molecular and Cellular Cardiology*, 52(6), 1213–1225. <https://doi.org/10.1016/j.yjmcc.2012.03.006>
- Siegel, R. L., Giaquinto, A. N., & Jemal, A. (2024). Cancer statistics, 2024. *CA: A Cancer Journal for Clinicians*, 74(1), 12–49. <https://doi.org/10.3322/caac.21820>
- Suk, J. S., Xu, Q., Kim, N., Hanes, J., & Ensign, L. M. (2016). PEGylation as a strategy for improving nanoparticle-based drug and gene delivery. *Advanced Drug Delivery Reviews*, 99, 28–51. <https://doi.org/10.1016/j.addr.2015.09.012>
- Sung, H., Ferlay, J., Siegel, R. L., Laversanne, M., Soerjomataram, I., Jemal, A., & Bray, F. (2021). Global cancer statistics 2020: GLOBOCAN estimates of incidence and mortality worldwide for 36 cancers in 185 countries. *CA: A Cancer Journal for Clinicians*, 71(3), 209–249. <https://doi.org/10.3322/caac.21660>
- Tacar, O., Sriamornsak, P., & Dass, C. R. (2013). Doxorubicin: An update on anticancer molecular action, toxicity and novel drug delivery systems. *Journal of Pharmacy and Pharmacology*, 65(2), 157–170. <https://doi.org/10.1111/j.2042-7158.2012.01567.x>
- Vejpongsa, P., & Yeh, E. T. H. (2014). Prevention of anthracycline-induced cardiotoxicity: Challenges and opportunities. *Journal of the American College of Cardiology*, 64(9), 938–945. <https://doi.org/10.1016/j.jacc.2014.06.1167>
- Wallace, K. B., Sardão, V. A., & Oliveira, P. J. (2020). Mitochondrial determinants of doxorubicin-induced cardiomyopathy. *Circulation Research*, 126(7), 926–941. <https://doi.org/10.1161/CIRCRESAHA.119.314681>
- Wilhelm, S., Tavares, A. J., Dai, Q., Ohta, S., Audet, J., Dvorak, H. F., & Chan, W. C. W. (2019). Analysis of nanoparticle delivery to tumours. *Nature Reviews Materials*, 1(5), 16014. <https://doi.org/10.1038/natrevmats.2016.14>
- Zhang, Y., Chan, H. F., & Leong, K. W. (2021). Advanced materials and processing for drug delivery: The past and the future. *Advanced Drug Delivery Reviews*, 65(1), 104–120. <https://doi.org/10.1016/j.addr.2012.10.003>
- Zhang, X., Li, F., Guo, S., & Gao, Y. (2022). pH-responsive liposomal nanocarriers for cancer therapy: Recent advances and challenges. *Acta Pharmaceutica Sinica B*, 12(5), 2023–2045. <https://doi.org/10.1016/j.apsb.2021.11.00>